Analytic Calculation of the DC-Link Capacitor Current for Pulsed Three-Phase Inverters

Folker Renken
Automotive Systems Powertrain
Siemens VDO Automotive AG
Siemensstraße 12
D-93055 Regensburg
Phone: ++49 941 790 5385 Fax: ++49 941 790 90541 E-Mail: folker.renken@siemens.com http://www.siemensvdo.com

Abstract - For pulsed three-phase inverters with symmetrical load the capacitor current in the dc-link circuit is analytically calculated. These calculations can be applied for a constant dc-voltage as well as for sinusoidal modulated voltages and sinusoidal currents at the output. The additional load of the dc-link capacitor caused by harmonic currents of the filter circuit or by switching transitions of semiconductors is examined, too. At last, the calculations are examined by practical measurements.

I. INTRODUCTION

Pulse inverters in uninterruptible power suppliers became generally accepted with the further development of disconnectible power semiconductors in the last years [1]. The dc-link capacitors contribute substantially to the volume, to the weight and to the costs of these inverters. For this reason the necessary expenditure of capacitors must be determined exactly to prohibit over design if possible. In most applications the dc-link capacitor effort is dependent on the load current. For pulsed three-phase inverters with symmetrical load the capacitor current in the dc-link circuit is analytically calculated. The power stage of the pulse inverter is presented in the following figure.

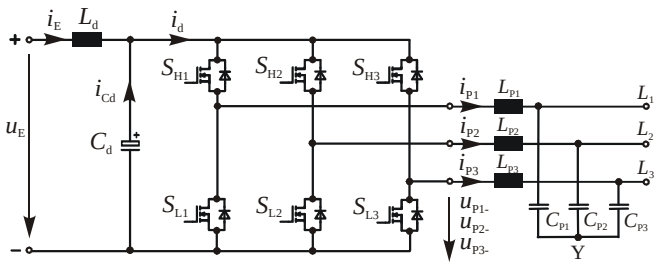

Fig. 1: Power stage of a pulsed three-phase inverter

The power stage consists out of three inverter-legs, an input filter circuit with dc-link capacitors and a three-phase filter circuit on the alternating voltage side.

II. PULSE CONTROL SCHEME OF THE INVERTER

For the calculation of the dc-link capacitor current, three sine-modulated phase voltages u_{P1-}, u_{P2-} and u_{P3-} are assumed, whose fundamental part has the same amplitude and a phase shift angle of 120° to each other. Beyond that a symmetrical load with any phase shift angle φ_{P1} as well as three-phase currents i_{P1}, i_{P2} and i_{P3} at the output of the inverter are presupposed. The dc-link voltage u_d at the dc-input of the inverter bridge is assumed as constant.

In figure 2 the pulsed control scheme of the three-phase inverter is presented. Above the three 120°-shifted sinusoidal control voltages u_{s1}, u_{s2}, and u_{s3} are compared with a higher frequency triangle shaped modulation voltage u_m. If one phase of the sinusoidal control voltages is higher than the modulation voltage the high-side switch of this phase is turned-on. In the other case the low-side switch of this bridge-leg is connected through. In this way the frequency of the

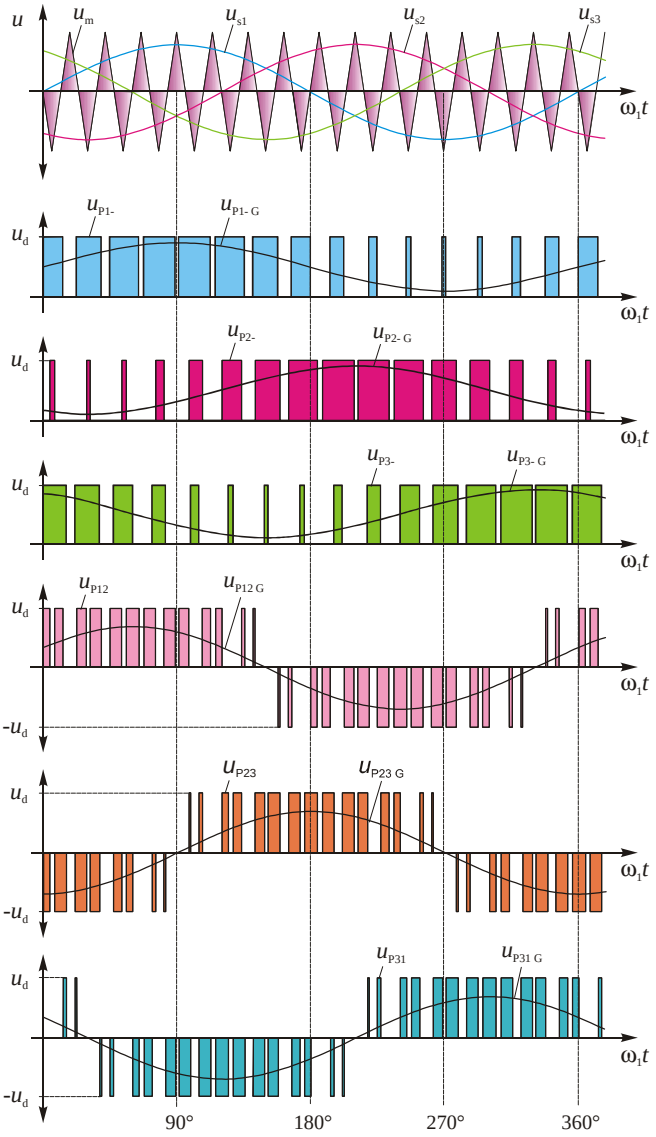

Fig. 2: Pulse control scheme of the three-phase inverter

triangle shaped modulation voltage u_m determines the pulse frequency of the inverter. The fundamental frequency is given by the frequency of the control voltages.

In the middle of the figure three half-bridge voltages u_{P1-}, u_{P2-}, and u_{P3-} with the fundamental oscillation frequency are shown. The lower part of the figure shows the connected voltages u_{P12}, u_{P23} and u_{P31} between the phases. It can clearly be seen - that with subtraction of the phase voltages during one period - two pulses are formed. These voltage waveforms at the load have approximately sinusoidal output currents in the individual phases of the inverter as consequence.

For ideal sinusoidal phase currents the generation of the input current i_d in a three-phase inverter is presented in figure 3. The modulation factor amounts thereby to m = 0.8 and the fundamental phase shift angle is $\varphi_{P1} = 45°$. Above the output voltages u_{P1-}, u_{P2-} and u_{P3-} are shown with the sinusoidal output currents i_{P1}, i_{P2} and i_{P3} of the inverter bridge-legs. These sinusoidal currents divide themselves in each case in the high side and low side transistor of the bridge-legs. In the figure the current pulses are shown, while the high side transistor of the respective bridge-leg leads. The sum of the current pulses of all three-phases results in the input current i_d of the inverter bridge.

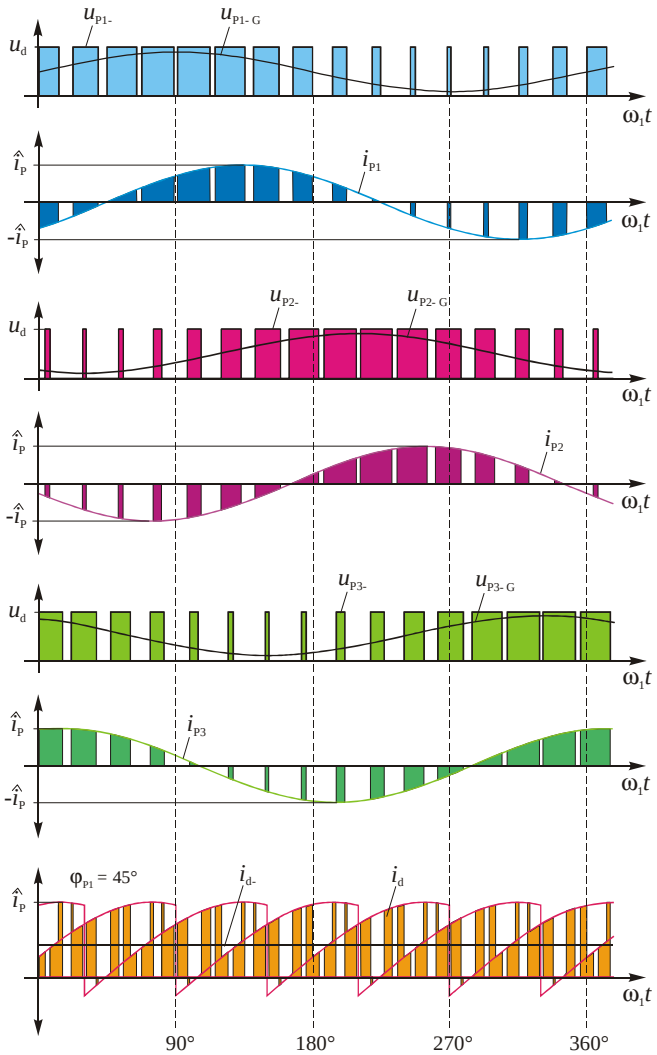

Fig. 3: Generation at the inverter bridge input current i_d

In figure 4 the pulse generation of the input current i_d in the inverter for different fundamental phase shift angles is presented. From the drawn envelopes it is clearly recognizable, that the waveforms of the curves after 1/6 of the fundamental period repeat always. The average value of the input current i_{d-} is positive with small phase shift angles (motor operation), equal to zero with $\varphi_{P1} = 90°$ and takes with larger angles to negative values (generator operation). The difference between the input current i_d and their average value i_{d-} flows in the dc-link capacitors [2].

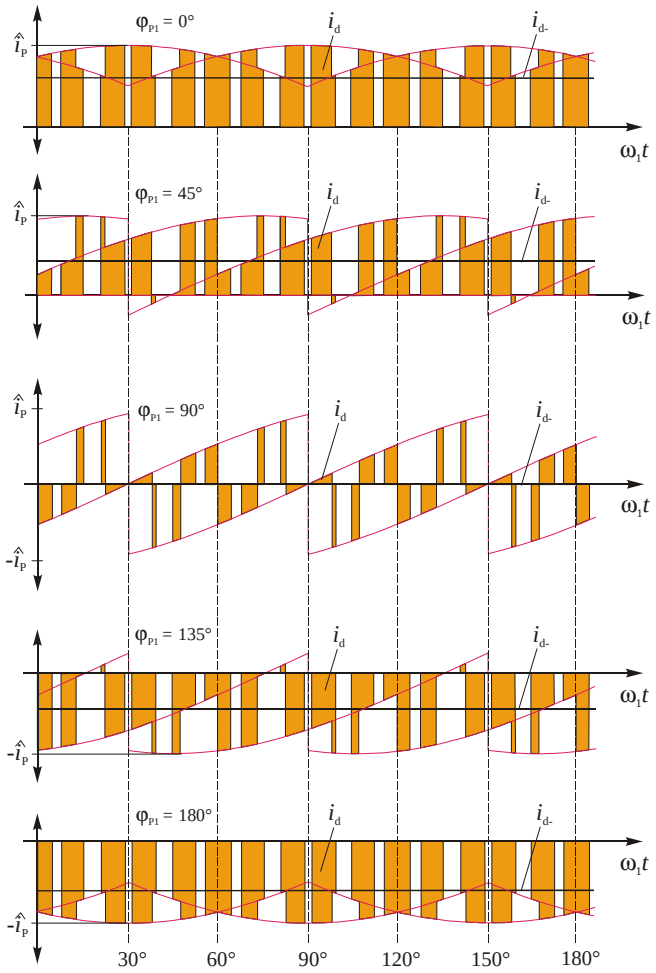

Fig. 4: Input current i_d with different phase shift angles φ_{P1}

III. CAPACITOR LOAD FOR SINE WAVE CURRENTS

Now the rms-current in the dc-link capacitors is analytically calculated for sine wave output currents with arbitrary phase shift angles f $_{P1}$ and modulation factors m. For this purpose the three sinusoidal desired waveforms u_{S1}, u_{S2} and u_{S3} are presented in the following illustration above. With pulse width modulation these three sinusoidal desired curves are compared with the triangle modulation voltage u_m. The frequency of the sinusoidal desired voltages determines the fundamental frequency and those of the modulation voltage the pulse frequency of the inverter.

It is presupposed that the pulse frequency of the inverter is very large, the three duty cycle curves follows in principle the same waveforms as the desired voltages, because of the comparison with the triangle modulation voltage (figure 5).

With the indicated duty cycle waveforms the output of the bridge-leg is connected in each case to the positive pole of the dc-input, so output current flows in the high side transistor of this bridge-legs.

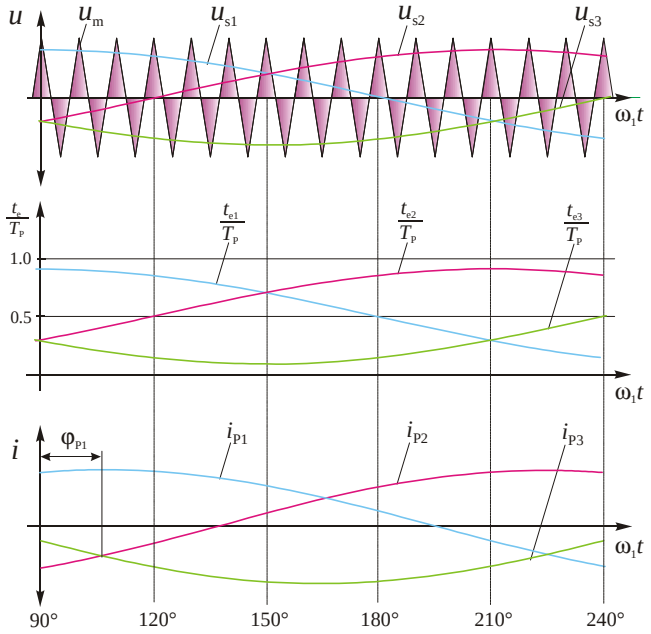

Fig. 5: Duty cycle waveforms and output currents of the three-phase inverter

Duty cycle waveforms of the phase voltages:

$$\frac{t_{e1}(t)}{T_P} = \frac{1}{2}\cdot\left[1+m\cdot\sin(\omega_1\cdot t)\right] \quad (1)$$

$$\frac{t_{e2}(t)}{T_P} = \frac{1}{2}\cdot\left[1+m\cdot\sin(\omega_1\cdot t-120°)\right] \quad (2)$$

$$\frac{t_{e3}(t)}{T_P} = \frac{1}{2}\cdot\left[1+m\cdot\sin(\omega_1\cdot t+120°)\right] \quad (3)$$

In the figure below the three currents at the output of the bridge-legs are presented. These currents all have the same amplitude and are shifted to the voltage by the same phase angle. (Symmetrical load).

Fundamental currents waveforms of the phases:

$$i_{P1}(t) = \hat{i}_P\cdot\sin\left(w_1\cdot t - j_{P1}\right) \quad (4)$$

$$i_{P2}(t) = \hat{i}_P\cdot\sin\left(w_1\cdot t - 120° - j_{P1}\right) \quad (5)$$

$$i_{P3}(t) = \hat{i}_P\cdot\sin\left(w_1\cdot t + 120° - j_{P1}\right) \quad (6)$$

As shown in chapter II the waveform of the bridge input currents i_d repeats after 1/6 of fundamental period. For this reason the dc-link current in the range 90° = ω t = 150° can be calculated. Within this range the following condition applies:

$$1 \geq \frac{t_{e1}(t)}{T_P} \geq \frac{t_{e2}(t)}{T_P} \geq \frac{t_{e3}(t)}{T_P} \quad (7)$$

Now for the elementary pulse period T_{PX} the input current i_d of the inverter within the range 90° = ω t = 150° is derived. In figure 6 the time durations of the different output currents in the high side switches of the bridge-legs in the elementary period T_{PX} is presented. Thereby altogether four time durations have to be differentiated.

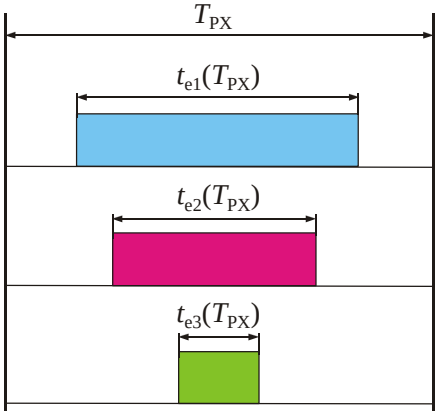

Fig. 6: The different time durations of the output currents in the high side switches at the pulse period T_{PX}

In table I the input currents in the different time durations of the elementary period T_{PX} of figure 6 are summarized. If all high side switches are in the blocking state, the current in the dc-input is zero. If only high side switch S_{H1} is turned on, the phase current i_{P1} flows in the dc-input. If the elements S_{H1} and S_{H2} switched on, the input current i_d can be calculated from the sum of phase current i_{P1} and i_{P2}. If all high side switches are switched on, then the current in the dc input consists out of the sum of all three-phase currents. With not connected neutral point the input current becomes zero.

Table I
Current i_d in the different time durations of T_{PX}

Time durations	Input current i_d:
$T_{PX} - t_{e1}(T_{PX})$	0
$t_{e1}(T_{PX}) - t_{e2}(T_{PX})$	$i_{P1}(T_{PX})$
$t_{e2}(T_{PX}) - t_{e3}(T_{PX})$	$i_{P1}(T_{PX}) + i_{P2}(T_{PX})$
$t_{e3}(T_{PX})$	$i_{P1}(T_{PX}) + i_{P2}(T_{PX}) + i_{P3}(T_{PX})$

Now all periods in the range 90° = ω t = 150° can be divided according like elementary period T_{PX} into time durations. If it is considered that the sum of the three currents at the output of the bridge-legs is zero, the time durations in all periods can be divided into three time durations with the following different current composition:

1. $$t_{e31}(t) = T_P - t_{e1}(t) + t_{e3}(t) \quad (8)$$
$$i_{d\,31}(t) = 0 \quad (9)$$

2. $$t_{e12}(t) = t_{e1}(t) - t_{e2}(t) \quad (10)$$
$$i_{d\,12}(t) = i_{P1}(t) \quad (11)$$

3. $$t_{e23}(t) = t_{e2}(t) - t_{e3}(t) \quad (12)$$
$$i_{d\,23}(t) = -i_{P3}(t) \quad (13)$$

with $$i_{P1}(t) + i_{P2}(t) + i_{P3}(t) = 0$$

The duty cycles can be calculated by the switching on times regarded to the elementary period T_P. Using the duty cycle and the current waveform during the fundamental period the three ranges results in the following equations:

1. $$\frac{t_{e31}(t)}{T_P} = 1 + \frac{\sqrt{3}}{2} \cdot m \cdot \cos(w_1 \cdot t + 60°) \quad (14)$$

$$i_{d31}(t) = 0 \quad (15)$$

2. $$\frac{t_{e12}(t)}{T_P} = \frac{\sqrt{3}}{2} \cdot m \cdot \cos(w_1 \cdot t - 60°) \quad (16)$$

$$i_{d12}(t) = \hat{i}_P \cdot \sin(w_1 \cdot t - j_{P1}) \quad (17)$$

3. $$\frac{t_{e23}(t)}{T_P} = -\frac{\sqrt{3}}{2} \cdot m \cdot \cos(w_1 \cdot t) \quad (18)$$

$$i_{d23}(t) = -\hat{i}_P \cdot \sin(w_1 \cdot t + 120° - j_{P1}) \quad (19)$$

Now with these equations the rms input current I_d of the inverter bridge can be determined. First the rms-value at the elementary pulse periods is determined (parentheses). The total rms-current can by calculated by integration of the rms-values of all pulse periods.

$$I_d = \sqrt{\frac{3}{p} \int_{w \cdot t = 90°}^{w \cdot t = 150°} \left\{ [i_{d12}(t)]^2 \cdot \frac{t_{e12}(t)}{T_P} + [i_{d23}(t)]^2 \cdot \frac{t_{e23}(t)}{T_P} \right\} dt} \quad (20)$$

$$I_d = \hat{i}_P \cdot \sqrt{\frac{m \cdot \sqrt{3}}{4 \cdot p} \cdot \left[1 + 4 \cdot \cos(j_{P1})^2 \right]} \quad (21)$$

The dc-component of the current flows over the dc input of the inverter bridge. This component can be calculated if at first the average value at the elementary pulse periods is determined (parentheses). Subsequently the average value within the range 90° = ω t = 150° will be determinate.

$$I_{d-} = \frac{3}{p} \int_{w \cdot t = 90°}^{w \cdot t = 150°} \left\{ [i_{d12}(t)] \cdot \frac{t_{e12}(t)}{T_P} + [i_{d23}(t)] \cdot \frac{t_{e23}(t)}{T_P} \right\} dt \quad (22)$$

$$I_{d-} = \frac{3}{4} \cdot \hat{i}_P \cdot m \cdot \cos(j_{P1}) \quad (23)$$

For ideally smoothed current in the dc-input of the inverter bridge i_E = i_{d-}, which occurs arises by the geometrical subtraction of total rms-current I_d and dc-component I_{d-} results in the current of the dc-link circuit capacitors.

$$I_{Cd} = \sqrt{I_d^2 - I_{d-}^2} \quad (24)$$

$$I_{Cd} = \hat{i}_P \cdot \sqrt{\frac{\sqrt{3} \cdot m}{4 \cdot p} + \left(\frac{\sqrt{3} \cdot m}{p} - \frac{9 \cdot m^2}{16} \right) \cdot \cos(j_{P1})^2} \quad (25)$$

The result shows: The rms-value of the current in the dc-link capacitors is depended on the modulation factor, the fundamental phase shift angle and the height of output current. The maximum rms-current in the dc-link capacitors mounts to:

$$I_{Cd} = \sqrt{\frac{25}{12 \cdot p^2}} \cdot \hat{i}_P \approx 0.46 \cdot \hat{i}_P \approx 0.65 \cdot I_P \quad (26)$$

with $j_{P1} = 0°$ and $m = \frac{10 \cdot \sqrt{3}}{9 \cdot p} \approx 0.613$

In figure 6 the current in the dc-link capacitors normalized to the peak value of output current as a function of the phase shift angle is presented for different modulation factors.

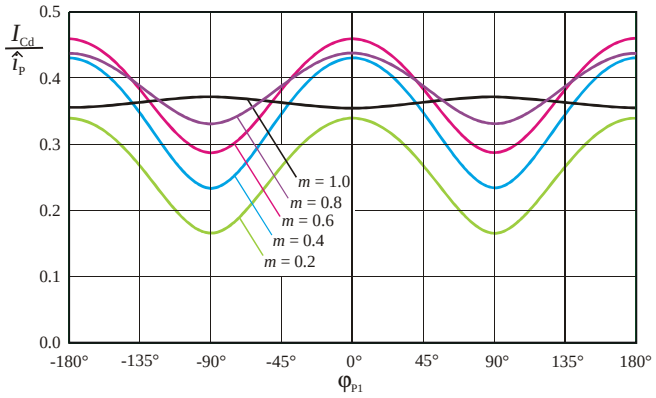

Fig. 7: Current in the dc-link capacitors as a function of the fundamental phase shift angle

It can clearly be recognized that with small modulation factors the load of the dc-link capacitor current is much larger with ohmic load as with inductive or capacitive load. With increasing modulation factor m the rms-value of the dc-link capacitor current for all phase angles φ_{P1} becomes larger. Only if the capacitor current with more rising modulation factor reaches its maximum, the current reduces again with ohmic load but with inductive or capacitive load continues to rise.

IV. CAPACITOR LOAD WITH HARMONICS

The calculated dc-link capacitor current in chapter III is made for a sinusoidal current i_P at the output of the inverter bridge. But by the pulse width modulated voltage however also harmonic current in the filter circuit occurs. This currents and the fundamental currents together forms the output current of the inverter bridge. The additional load in the dc-link capacitors of these higher-frequency currents must to be determined with the help of the Fourier analysis.

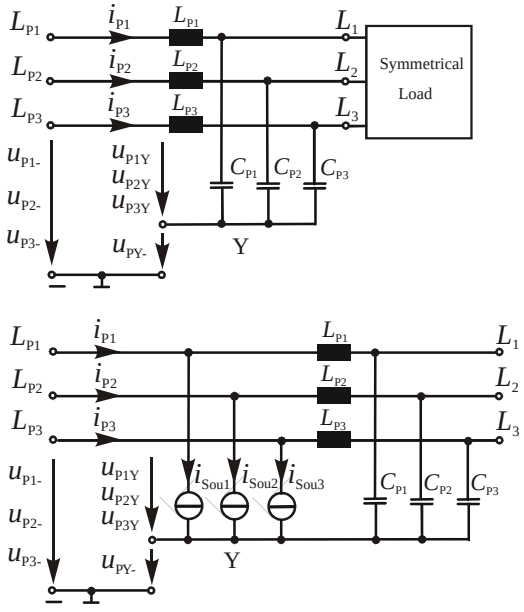

Fig. 8: Filter circuit with symmetrical load (above) and filter circuit with zero load and substitute load at the input (below)

In figure 8 (above) the filter circuit of the three-phase inverter is presented. During the design of the filter circuit elements a compromise between large losses with large inductance and small capacity as well as with better rule dynamics of the inverter with small inductance and large filter circuit capacity must be reached. For the inductance design it is usual to use the permissible maximum current in the inductance during the pulse period referred to the peak value of the nominal output current.

$$\Delta i_{\mathrm{LP\ max}} = (0.1 - 0.3) \cdot \hat{i}_{\mathrm{AN}} \tag{27}$$

The harmonic current which is limited by the inductance, flow over the capacitor and produces a voltage ripple which is superimposing the output voltage. This static voltage ripple is specified to a maximum permissible value by the design of the filter capacity. A maximum voltage ripple of smaller than 1% of the peak value of the output voltage is usual [3].

$$\Delta u_{\mathrm{AP\ max}} \leq 0.01 \cdot \hat{u}_{\mathrm{AN}} \tag{28}$$

For this small voltage ripple during the pulse periods sinusoidal voltage and current waveforms at the output of the filter can be accept in very good approximation. The sinusoidal current at the output forms together with the filter capacitor currents the output current of the bridge-legs.

Now for the calculation of the input current i_d the currents in the bridge-legs are to be derived. For this the alternate filter circuit is presented in the figure 8 below. In this mathematical model the filter circuit of the inverter is without load, so that only the idle current flows in the filter circuit. The load of the inverter is reproduced thereby by the current sources arranged parallel to the filter circuit. The following equation shows the current waveform in the source of phase 1.

$$i_{\mathrm{Sou1}}(t) = \hat{i}_{\mathrm{Sou}} \cdot \sin(\omega_1 \cdot t - \varphi_{\mathrm{Sou}}) \tag{29}$$

The current waveforms of the other sources have a phase angle of 120° to the current in equation 29, so that all sources together forms a symmetrical load. The addition of the currents of filter circuit and current sources results in the output current of the bridge-legs. For the calculation of the dc-link capacitor current first the pulse signal presented in the following figure is to be mathematically described with the help of the Fourier analysis.

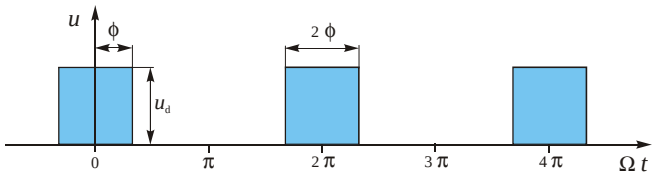

Fig. 9: Pulse waveform with constant pulse width

In the figure a pulse waveform with the constant pulse width 2ϕ and the height u_d is presented. This waveform can be mathematically described by the following functions [4].

$$u(\Omega t) = \frac{2 \cdot u_{\mathrm{d}}}{\pi} \cdot \left[\frac{\phi}{2} + \frac{\sin(\phi)}{1} \cdot \cos(\Omega t) + \frac{\sin(2 \cdot \phi)}{2} \cdot \cos(2 \cdot \Omega t) + \ldots \right] \tag{30}$$

$$u(\Omega t) = \frac{2 \cdot u_{\mathrm{d}}}{\pi} \cdot \left[\frac{\phi}{2} + \sum_{\mu=1}^{\infty} \frac{1}{\mu} \cdot \sin(\mu \cdot \phi) \cdot \cos(\mu \cdot \Omega t) \right] \tag{31}$$

With the pulse width modulation the pulse width 2ϕ changes over the fundamental period. This is shown by the duty cycle waveform in equation 1. With this function the waveform of the pulse width $2\phi(w_1 t)$ can be determined.

$$\phi(\omega_1 t) = \pi \cdot \frac{t_{\mathrm{e1}}}{T_{\mathrm{P}}} = \frac{\pi}{2} + \frac{\pi \cdot m}{2} \cdot \cos(\omega_1 t) \tag{32}$$

The pulse waveform in an elementary period is indicated by the size Ωt. This size can be calculated as a function of the fundamental period $\Omega t(w_1 t)$. The factor ρ indicates the number of pulses per fundamental period $\rho = w_P/w_1$.

$$\Omega t(\omega_1 t) = 2 \cdot \pi \cdot \frac{t}{T_{\mathrm{P}}} = \omega_{\mathrm{P}} \cdot t = \rho \cdot \omega_1 \cdot t \tag{33}$$

These equations now result in the voltage waveform of the pulse width modulated signal at the output of the bridge-legs. The variable π in the cosine function indicates the phase shift angle of the pulses in the pulse periods. The height of the voltage pulses amounts to u_d.

$$u_{\mathrm{P1-}}(\omega_1 t) = u_{\mathrm{d}} \cdot \left\{ \frac{1}{2} \cdot [1 + m \cdot \cos(\omega_1 t)] + \right. \tag{34}$$

$$\left. \sum_{\mu=1}^{\infty} \frac{2}{\mu \cdot \pi} \cdot \sin\left[\frac{\mu \cdot \pi}{2} \cdot [1 + m \cdot \cos(\omega_1 t)] \right] \cdot \cos[\mu \cdot (p \cdot \omega_1 t + \pi)] \right\}$$

In figure 10 the half bridge voltage u_{P1-} and their fundamental portion is presented. The modulation factor of this voltage amounts to $m = 0.8$ and the pulse number per fundamental period is $\rho = 45$. Below in the figure the spectra of this half bridge voltage can be seen. The standardized dc-component of the voltage amounts to 0.5 and the fundamental component are according to the modulation factor equal 0.8. Beyond that by the modulation of the voltage in each case frequency bands occurs with the pulse frequency and with multiples of the pulse frequency. All harmonics of the waveform are odd.

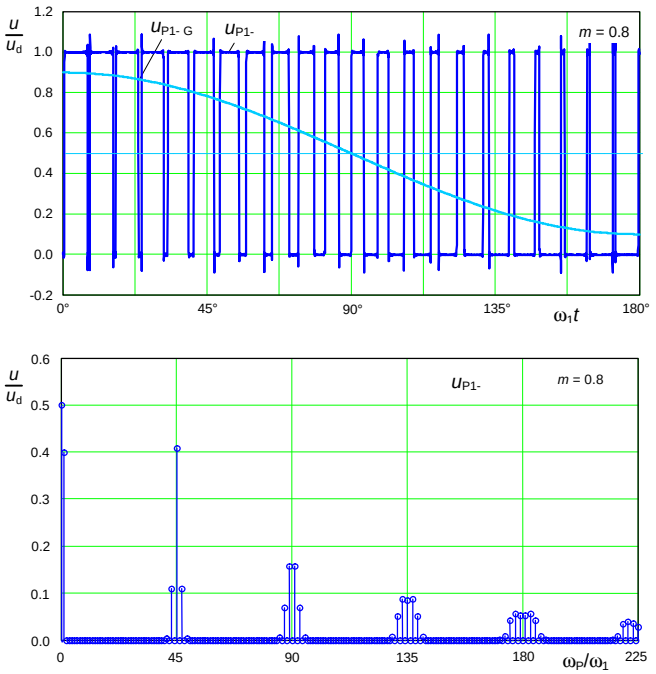

Fig. 10: Half-bridge voltages u_{P1-} with the fundamental oscillation frequency u_{P1-G}

The voltage at the neutral point u_{PY-} can be determined as the sum of all three half bridge voltages divided by three. To calculate this voltage first the voltage u_{P2-} and u_{P3-} must be determined. These voltages have a phase angle of 120° to the voltage u_{P1-}. However it must be noted with the calculation that the pulse position is equal. For this reason the expression $\rho\omega_1 t$ must stay unchanged. In such a way the same pulse position is reached as shown in figure 2 and 3.

$$u_{PY-}(w_1 t) = \frac{1}{3} \cdot \left[u_{P1-}(w_1 t) + u_{P2-}(w_1 t) + u_{P3-}(w_1 t) \right] \quad (35)$$

$$u_{PY-}(w_1 t) = \frac{1}{3} \cdot \left[u_{P1-}(w_1 t) + u_{P1-}(w_1 t - 120°) + u_{P1-}(w_1 t + 120°) \right] \quad (36)$$

The following figure shows the calculated waveform of the neutral point voltage u_{PY-} with the average value for the modulation factor m = 0.8 and for the pulse number ρ = 45. Below in the figure again the individual spectra of the voltage are presented. The standardized dc-component of the voltage amounts to 0.5. Furthermore, with this voltage all by three dividable spectra from figure 10 arises.

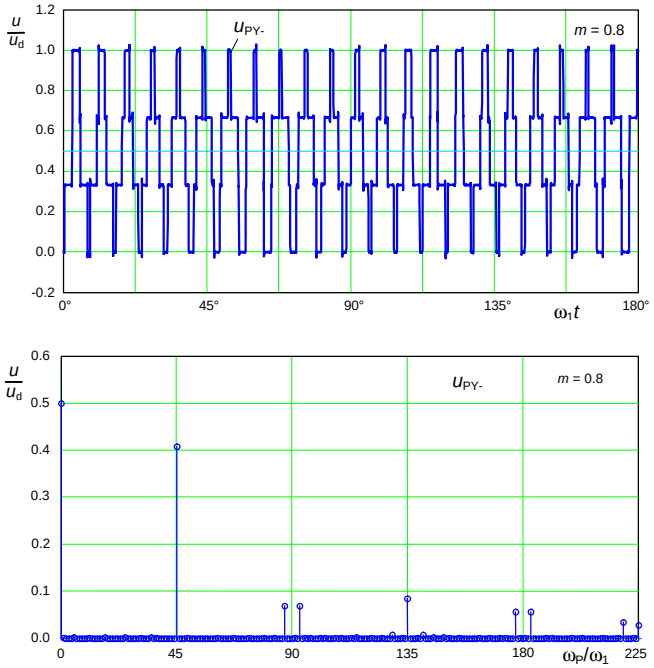

Fig. 11: Neutral point voltage u_{PY-} with the average value

The phase voltage u_{P1Y} is the difference between half bridge - and neutral point voltage. Exactly as with the calculation of the neutral point voltage there also must paid attention to the correct phase shift angle and pulse position.

$$u_{P1Y}(w_1 t) = u_{P1-}(w_1 t) - u_{PY-}(w_1 t) \quad (37)$$

$$u_{P1Y}(w_1 t) = \frac{1}{3} \cdot \left[2 \cdot u_{P1-}(w_1 t) - u_{P1-}(w_1 t - 120°) - u_{P1-}(w_1 t + 120°) \right] \quad (38)$$

To calculate the phase current i_{P1} with the voltage u_{P1Y} the cosine function in the argument of the sine - and cosine functions by means of the Bessel functions must be dissolved. The following relations apply:

$$\sin[a \cdot \cos(b)] = \sum_{n=0}^{\infty} \sin\left(\frac{n \cdot p}{2}\right) \cdot k_n \cdot J_n(a) \cdot \cos(n \cdot b) \quad (39)$$

$$\cos[a \cdot \cos(b)] = \sum_{n=0}^{\infty} \cos\left(\frac{n \cdot p}{2}\right) \cdot k_n \cdot J_n(a) \cdot \cos(n \cdot b) \quad (40)$$

with $$k_n = \begin{cases} 1 & \text{if } n = 0 \\ 2 & \text{if } n = 1, 2, 3, \ldots \end{cases}$$

With the help of these Bessel functions now first the phase voltage u_{P1Y} can be calculated. With the result that in the following equation is presented the individual spectra are recognizably. This makes the following calculation of the phase current possible.

$$u_{P1Y}(w_1 t) = \frac{U_d \cdot m}{2} \cdot \cos(w_1 t) + \quad (41)$$

$$\sum_{\mu=1}^{\infty} \sum_{\nu=0}^{\infty} \left\{ \frac{2 \cdot U_d}{3 \cdot \pi \cdot \mu} \cdot \left[1 - \cos\left(\frac{2 \cdot \pi \cdot \nu}{3}\right) \right] \cdot \sin\left(\frac{\pi \cdot (\mu + \nu)}{2}\right) \cdot k_\nu \cdot J_\nu\left(\frac{\pi \cdot \mu \cdot m}{2}\right) \cdot \left[\cos[(\mu \cdot \rho - \nu) \cdot \omega_1 + \mu \cdot \pi] + \cos[(\mu \cdot \rho + \nu) \cdot \omega_1 + \mu \cdot \pi] \right] \right\}$$

With the determination of the phase current i_{P1} the individual voltage components are in each case divided by the absolute value of the resistance and provided with the appropriate phase shift angle. For the fundamental component from the equation 41 only the "no-load" operation of the filter circuit is considered. As additional fundamental load the current source i_{Sou1} is used as shown in figure 8.

$$i_{P1}(\omega_1 t) = \hat{i}_{Sou} \cdot \sin(\omega_1 \cdot t - \varphi_{Sou}) + \frac{U_d \cdot m}{2 \cdot |Z_{PF}|} \cdot \cos(\omega_1 t - \varphi_{PF}) + \quad (42)$$

$$\sum_{\mu=1}^{\infty} \sum_{\nu=0}^{\infty} \left\{ \frac{2 \cdot U_d}{3 \cdot \pi \cdot \mu} \cdot \left[1 - \cos\left(\frac{2 \cdot \pi \cdot \nu}{3}\right) \right] \cdot \sin\left(\frac{\pi \cdot (\mu + \nu)}{2}\right) \cdot k_\nu \cdot J_\nu\left(\frac{\pi \cdot \mu \cdot m}{2}\right) \cdot \left[\frac{1}{|Z_{PO-}(\mu, \nu)|} \cdot \cos[(\mu \cdot \rho - \nu) \cdot \omega_1 + \mu \cdot \pi - \varphi_{PO-}(\mu, \nu)] + \frac{1}{|Z_{PO+}(\mu, \nu)|} \cdot \cos[(\mu \cdot \rho + \nu) \cdot \omega_1 + \mu \cdot \pi - \varphi_{PO+}(\mu, \nu)] \right] \right\}$$

In equation 42 the following absolute values of the resistances Z_{P1} and $Z_{PO\pm}(\mu, \upsilon)$ as well as the phase shift angles j_{P1} and $j_{PO\pm}(\mu, \upsilon)$ are to be used:

$$|Z_{PF}| = \sqrt{R_{LP}^2 + \left(2 \cdot \pi \cdot L_P - \frac{1}{2 \cdot \pi \cdot C_P}\right)^2}$$

$$\varphi_{PF} = \arctan\left(\frac{2 \cdot \pi \cdot L_P - \frac{1}{2 \cdot \pi \cdot C_P}}{R_{LP}} \right)$$

$$|Z_{PO\pm}(\mu, \nu)| = \sqrt{R_{LP}^2 + \left[(\mu \cdot \rho \pm \nu) \cdot 2 \cdot \pi \cdot L_P - \frac{1}{(\mu \cdot \rho \pm \nu) \cdot 2 \cdot \pi \cdot C_P} \right]^2}$$

$$\varphi_{PO\pm}(\mu, \nu) = \arctan\left[\frac{(\mu \cdot \rho \pm \nu) \cdot 2 \cdot \pi \cdot L_P - \frac{1}{(\mu \cdot \rho \pm \nu) \cdot 2 \cdot \pi \cdot C_P}}{R_{LP}} \right]$$

In figure 12 the phase voltage u_{P1Y} and the phase current i_{P1} is presented with half nominal load and with a phase shift angle of φ_{P1} = 45°. The fundamental current with superimposed harmonics, is clearly recognizable thereby. In the figure below

the individual spectra of the voltage u_{P1Y} and the current i_{P1} can to be seen.

From the spectra presented in figure 10 only the not by three divisible voltage spectra remain. Each of these harmonics produced a current in the filter circuit. The more largely the harmonic is the more the current is absorbed by the filter circuit.

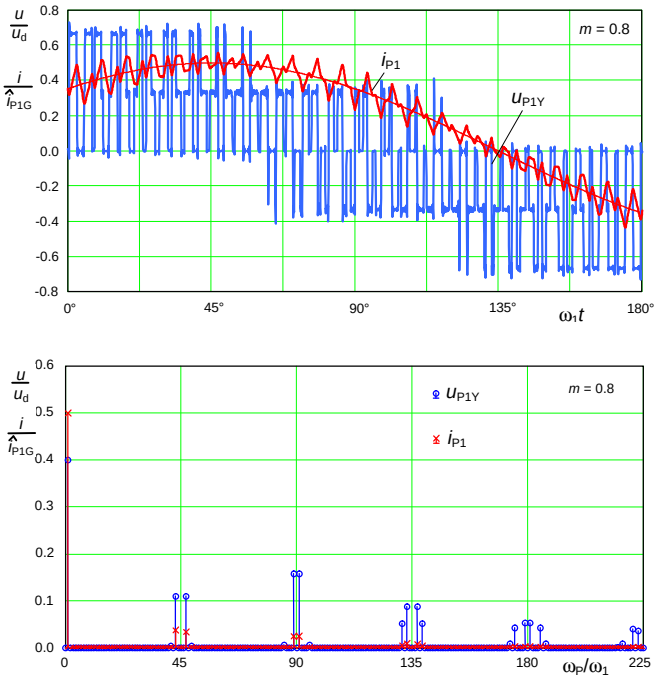

Fig. 12: Voltage u_{P1Y} at the load and the output current i_{P1} without and with harmonics ($\varphi_{P1} = 45°$)

With the phase current and the output voltages of the bridge-legs now the current i_d in the input of the inverter bridge can be calculated. As graphically presented in figure 3, the respective phase current is thereby multiplied in each case by the appropriate pulse pattern of the bridge-leg voltages and the results afterwards added. For this calculation first the currents i_{P2} and i_{P3} and the voltages u_{P2-} and u_{P3-} must be derived. These currents have a phase shift angle of 120° to the current i_{P1} and the voltages to voltage u_{P1-}. However here in the calculation it must be noted that the pulse position is equal. For this reason the expression $\rho\omega_1 t$ must remain unchanged. In such a way the same pulse position can be reached as presented in figure 3.

$$i_d(\omega_1 t) = i_{P1}(\omega_1 t)\cdot\frac{u_{P1-}(\omega_1 t)}{u_d} + i_{P2}(\omega_1 t)\cdot\frac{u_{P2-}(\omega_1 t)}{u_d} + i_{P3}(\omega_1 t)\cdot\frac{u_{P3-}(\omega_1 t)}{u_d} \quad (43)$$

$$i_d(\omega_1 t) = i_{P1}(\omega_1 t)\cdot\frac{u_{P1-}(\omega_1 t)}{u_d} + i_{P1}(\omega_1 t - 120°)\cdot\frac{u_{P1-}(\omega_1 t - 120°)}{u_d} + \quad (44)$$

$$i_{P1}(\omega_1 t + 120°)\cdot\frac{u_{P1-}(\omega_1 t + 120°)}{u_d}$$

In figure 13 the current i_d is presented for a sinusoidal phase current i_P and a phase shift angle $\varphi_{P1} = 45°$. This curve of the current corresponds in principle to the drawn waveform of i_d in figure 3. However number of the pulses ($\rho = 45$) is larger in this example. The course of the curve repeats in each case after 1/6 of the fundamental period. This is also shown by the spectra in the figure below, which are divisible by six in each case. The dc-component corresponds to equation 23 (half nominal current). Beyond that, frequency bands occur with the pulse number and with multiples of the pulse numbers.

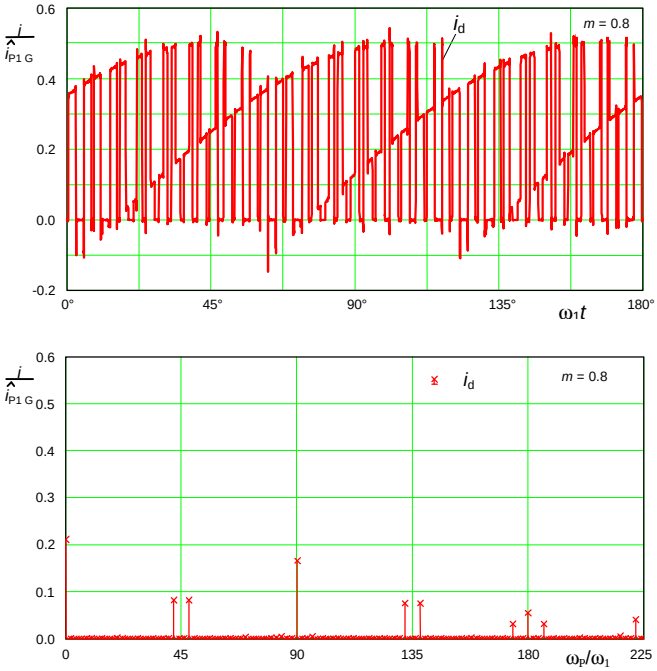

Fig. 13: Current i_d in the dc-link circuit without harmonic output current ($\varphi_{P1} = 45°$)

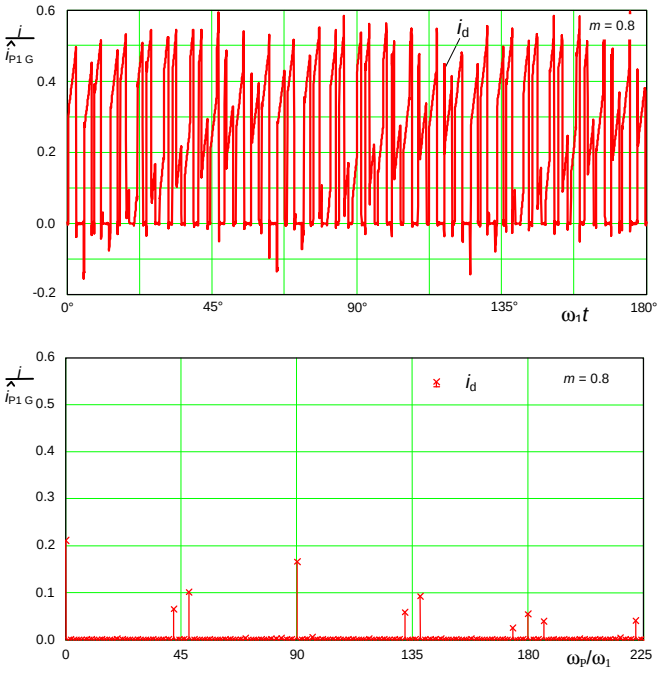

Fig. 14: Current i_d in the dc-link circuit with harmonic output current ($\varphi_{P1} = 45°$)

In figure 14 the current i_d is presented with superimposed harmonic phase currents i_P. The phase shift angle of the fundamental waveform is $\varphi_{P1} = 45°$. In opposite to the curve in which is presented figure 13 still another additional higher frequency current is superimposed to the already with harmonics influenced input current. The course of the curve

repeats also here in each case after 1/6 of the fundamental period. This is shown at the spectra, which are presented in the figure below.

Now the influence of the harmonic filter currents (figure 12) to the load of dc-link capacitor is calculated. Thereby it is presupposed, that an ideally dc-current flow $i_E = i_{d-}$ in the input of the inverter (worst case). So the individual input current harmonic components of the inverter bridge can be calculated in each case with sinusoidal phase currents and with harmonic filter current that are superimposing the sinusoidal components. At first the rms-values of the amplitudes of all harmonics in equation 45 are to be derived and then the calculated individual portions are added geometrically.

$$I_d = \sqrt{\sum_{n=1}^{\infty}\left(\frac{\hat{i}_{Cd\,n}}{\sqrt{2}}\right)^2} \qquad (45)$$

The calculations with additional harmonic filter currents are related to them with sinusoidal current. In figure 15 the results from the calculations as a function of the load are presented with different modulation factors. The maximum current ripple specified by the dimensioning of the filter circuit amounts in this case to 0.3 $\hat{i}_{AN}$. In the following figure the influence of the harmonic filter circuit current is presented with $\varphi_1 = 0°$ (above) and with $\varphi_1 = 45°$ (below).

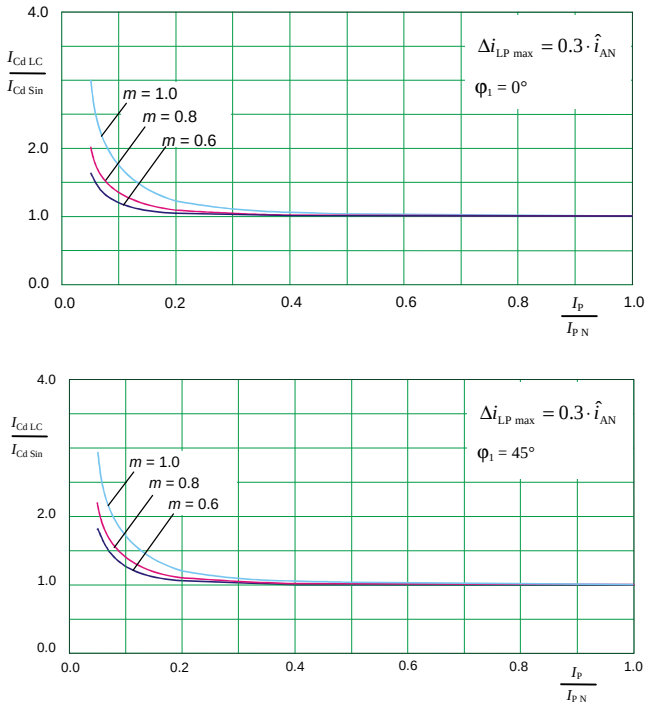

Fig. 15: Influence of the harmonic output filter current on the dc-link capacitor current

In the figure is clearly recognizable, that the harmonic ripple current of the filter circuit only stresses the dc-link capacitors considerable with small output currents $i_P < 0.3\,i_{AN}$ additionally. With larger output current the dc-link capacitor load corresponds to that with sinusoidal output current of the inverter bridge in very good approximation. For the dimensioning of the capacitors in the dc-link circuit for instance, these large loads are important. That means that sinusoidal output currents for the dimensions of the dc-link capacitors are sufficient. The load of the capacitors for sinusoidal output currents was presented in figure 7.

Beside the harmonious currents at the filter circuit still current harmonics arise by switching processes in the bridge-legs. This current was examined in [5, 6, 7] for single-phase inverters. The tendentious results have also their validity for a three-phase inverter. With small output load of the inverter the additional current of the switching processes in the dc-link circuit can substantially contribute to heating up of the dc-link capacitors. During higher load usually again the calculated by sine wave output current caused capacitor current dominated. But no statement for all semiconductor types can be made. Beyond that this additional current contributed considerably by the pulse frequency of the inverter.

V. COMPARSION OF THE CALCULATIONS WITH PRACTICAL MESUREMENTS

Now the calculated capacitor current in the dc-link circuit is to be compared with practical measurements of a MOSFET-inverter. The dc-link circuit of the inverter consists out of 7 electrolytic capacitors. For the 6 switches in each case 8 MOSFETs are connected in parallel. The inverter works with a pulse frequency of $f_P = 8$ kHz. The nominal output power of the inverter in continuous operation amounts to $P_N = 6$ kW and the input voltage is $u_d = 48$V [8, 9, 10]. At the inverter output an electrical machine is attached, which can work both in the motor and in the generator operation.

The currents in the individual capacitors of the dc-link circuit are measured with current probes, whereby the individual measured values are transfer over current transformers at first. The waveforms of the individual capacitor currents are presented and the rms-values are calculated with the oscilloscope.

Figure 16 above shows the current waveforms in three capacitors of the inverter with an output current of $I_P = 158$A and with a phase shift angle of $\varphi_{P1} = 130°$. At this phase angle the electrical machine works in the generator operation.

The rms-value of the current in each individual capacitor amounts to $I_{Cd1} \approx 12$A. Beyond that the respective portions of the peak output current $\hat{i}_{P\,1} \approx 32$A and of the dc-current $I_{d-\,1} \approx -12$A can be seen in the diagram waveforms apart from the period duration $T_1 \approx 10.2$ms. The sum of the current components in all 7 capacitors results in each case in the total current value. Below the current diagrams the most important electrical parameter of the inverter are presented.

Below in the figure the current waveforms in the individual capacitors with an output current of $I_P = 238$A and a phase shift angle of $\varphi_{P1} = 125°$ are presented. During this mode the rms-current in each individual capacitors amounts to $I_{Cd1} \approx 18.5$A. The duration of the fundamental period is $T_1 \approx 11.8$ms, each peak value of output current is $\hat{i}_{P\,1} \approx 48$A

and each input dc-current is $I_{d-1} \approx$ -19A. Below the current waveforms also the most important electrical parameters of the inverter are presented.

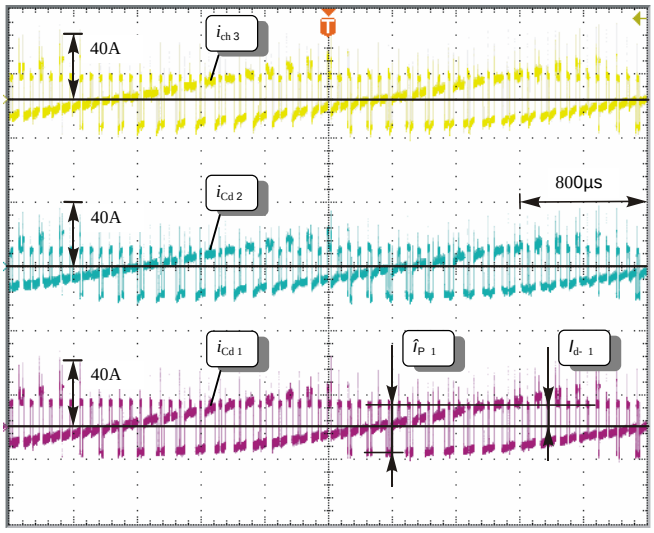

U_{PY} = 13.9 V U_d = 48 V f_1 = 100 Hz φ_{P1} = 130°

I_P = 158 A I_{d-} = -86 A I_{Cd} = 84 A m = 0.8

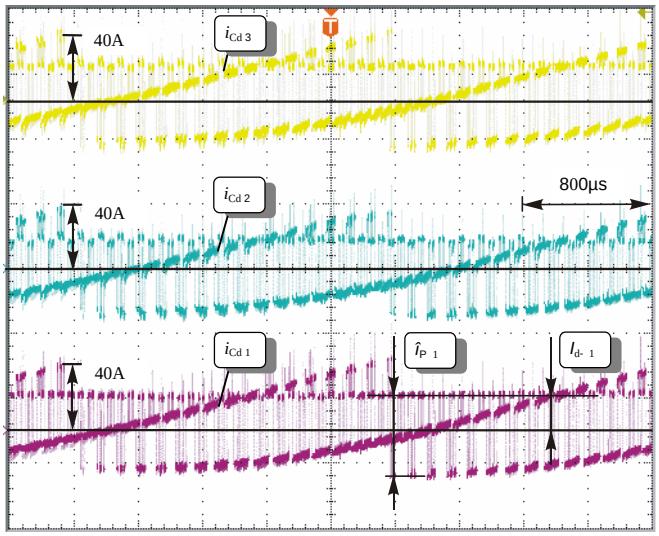

U_{PY} = 15.7 V U_d = 48 V f_1 = 85 Hz φ_{P1} = 125°

I_P = 238 A I_{d-} = -130 A I_{Cd} = 124 A m = 0.9

Fig. 16: Current in three dc-link capacitors of the inverter with different loads (practical measurements)

The current of the practical measurements corresponds in principle to the waveforms of the capacitor current in figure 3. The rms-value of this current depends to the size of output current, on the phase shift angle and of the modulation factor. The rms-value of the capacitor current is the same as the calculated current which is presented in figure 7.

VI. CONCLUSION

Today pulse inverters are used world-wide within many ranges for ac power supply, for drive train engineering and for frequency conversion. The dc-link capacitor in the power parts contributes thereby substantially to the volume, to the weight and to the costs of such inverters. For this reason the necessary size of capacitors must be determined exactly to avoid over design. In most applications the dc-link capacitor size is dependent by the current load.

In this publication the dc-link capacitor current for a three-phase inverter was analytically calculated. At first an ideal smoothed input dc-voltage as well as sinusoidal currents at the output of the inverter bridge is presupposed. The results show that the input current of the inverter bridge consists out of a dc-component with higher-frequency portions.

While the dc-component flows in the input of the inverter, the higher-frequency current portion in reality flows completely over the dc-link circuit capacitor. This portion can amount maximally to a value $I_{Cd} = 0.46\ \hat{i}_P$.

In chapter IV the influence by current harmonics, which result from the output filter circuit and from switching processes in the inverter bridge is examined. It shows that with small output power a clear capacitor load results by these harmonics. But with higher output power again the calculated load caused by sine wave current dominates. The load of the dc-link capacitors by this harmonics can be neglected.

At the end the calculated dc-link currents are compared with practical measurements of an MOSFET inverter. The current of the practical measurements corresponds in principle to the theoretical waveforms. Beyond that a very good agreement between the calculated and measured values exists.

REFERENCES

[1] J. Schmidt, "Einsatzbereiche, Anforderungen und Konzepte netzunabhängiger Stromversorgungen," Seminar Haus der Technik e.V. Essen 1999

[2] K. Heumann, "Grundlagen der Leistungselektronik," Lehrbuch Teubner Verlag Stuttgart 1975, 1. Auflage S. 178-182

[3] F. Renken, "Einphasige Wechselrichter mit hart und weich schaltenden Transistoren für statische unterbrechungsfreie Stromversorgungen", Dissertation Univ. der Bw. Hamburg, VDI Verlag 1999, Fortschritt-Berichte ISBN 3183271214, S. 35-82

[4] H.-J. Bartsch, "Taschenbuch mathematischer Formeln," Harry Deutsch Verlag 1982, 6. Auflage S. 413

[5] F. Renken, "Analytic Calculation of the DC-Link Capacitor Current for Pulsed Single-Phase H-Bridge Inverters", 10th EPE Toulouse 2003

[6] F. Renken, "Analytic Calculation of the DC-Link Capacitor Current for Pulsed Single Phase H-Bridge Inverters", EPE Journal Volume 13 – No 4 - September - October - November 2003

[7] Renken F. "Inverter with Soft-Switched Transistors for Uninterruptible Power Supplies", 10. EPE Meeting/ Proceedings: Papers on CD ISBN 90-75815-07-7, Toulouse, France 2003

[8] V. Karrer, F. Renken, "Power Electronics for the Integrated Starter Generator", Conference: Optimization of the power train in vehicles by using the Integrated Starter Generator (ISG), Haus der Technik e. V. Munich 2002, Proceedings Expert-Verlag ISBN 3-8169-2977-2, pp. 222-247

[9] F. Renken, V. Karrer, "Leistungselektronik für den Integrierten Starter Generator," 22. Tagung Elek-tronik im Kraftfahrzeug", Haus der Technik – Essen, Tagungs-Nr. E-H030-06-056-2, Stuttgart 2002

[10] Skotzek P., Reindl T., Poisel M., Eichenseher V., Karrer V., Allwang R.: Steuergerät für den Integrierten Starter Generator im 42V-Bordnetz. 21. Tagung „Elektronik im Kraftfahrzeug“, Haus der Technik - Essen, München Mai 2001